Proceedings of CECNet 2022
A.J. Tallón-Ballesteros (Ed.)

doi:10.3233/FAIA220551

Low Complexity and High Spectrum Efficiency Hybrid Precoding for Massive MIMO Systems

Gang XIE[1] and Zhixiang PEI
School of Information and Communication Engineering, Beijing University of Posts and Telecommunications, Beijing 100876, China.

Abstract. Recently, alternating minimization has been widely employed for hybrid fully-connected precoding schemes, whereas the complexity is too high. In order to further reduce the complexity while maintaining the performance of single user point-to-point millimeter wave multiple-input multiple-output (MIMO) systems, we propose an alternating minimization algorithm of inverse matrix's phase extraction based on orthogonal matching pursuit (AIPO). Firstly, both the analog and digital precoding matrices are obtained by orthogonal matching pursuit algorithm. Then, the analog precoding matrix is updated using the phase information extracted from the digital precoding matrix and the optimal digital precoding matrix. Finally, the local optimal solution can be iteratively obtained under the least squares criterion and the modulus constraint. Simulation results verify that the proposed algorithm is capable of dramatically decreasing the complexity by more than sixty percent without compromising spectrum and energy efficiencies.

Keywords. Hybrid precoding, alternating minimization, MIMO, AIPO

1. Introduction

The past few years have witnessed the rapid growth of global demand for wireless data traffic. However, due to limited spectrum resources, it is rather overwhelming for fifth-generation (5G) mobile communication systems to meet the increasing demands of users for an ultra-high data rate. Therefore, the exploitation of unauthorized millimeter wave band for communication has attracted widespread attentions from both domestic and foreign scholars. Thanks to the relatively short wavelength of millimeter wave, the physical size of antenna array is greatly reduced, thereby implying that large-scale antenna can be deployed at the base station. In line with this insight, it is intuitive to jointly combine millimeter wave with massive MIMO in an efficient manner.

Hybrid precoding technology is one of the most promising technologies in millimeter wave massive MIMO system [1]. So far, the research on hybrid precoding mainly focuses on two kinds of structures: fully connected structure [2-5] and partially connected structure [6-7]. For the fully connected hybrid precoding structure, each RF link connects to all antennas. The hybrid precoding for this structure can obtain all beamforming gains, which achieves comparable performance digital precoding.

[1] Corresponding author: Xie Gang, Beijing University of Posts and Telecommunications; E-mail: xiegang@bupt.edu.cn

Nevertheless, the disadvantages of this structure primarily include high complexity and power consumption. For the partially connected structure, each RF link merely connected to a part of the antennas. As a result, it only obtains incomplete beamforming gain, which thus compromises the performance. In order to improve the spectrum efficiency as much as possible, we consider full connection structure in this paper.

To improve the low spectral efficiency of existing communication systems, a hybrid precoding algorithm based on orthogonal matching pursuit (OMP) was proposed in [1]. The algorithm improved the spectrum efficiency to a certain extent. However, limited by the feasibility of the analog precoding matrix, performance loss is inevitable. To acquire a high spectrum efficiency, Yu. proposed propose a manifold optimization based AltMin (MO-AltMin) algorithm [8]. The spectrum efficiency was greatly improved under this algorithm, which is sufficiently close to the optimal digital precoding. However, it has to endure a heavy computational complexity to find the global optimal precoding matrix.

In order to reduce the unnecessary complexity, a phase extraction based alternating minimization (PE-AltMin) algorithm was proposed in [8]. Compared with MO-AltMin, this algorithm greatly reduces the complexity while maintaining the same spectrum efficiency. However, this algorithm can only guarantee a local optimal solution, and the convergence behavior over the iterations can be poor.

What this paper aims to do is to reduce the number of iterations after achieving a better result, and then reduce the complexity of each iteration by simple multiplication and division, thus reducing the computational complexity of the whole algorithm while maintaining the system performance.

2. System Model

2.1. Fully Connected Hybrid Precoding System

We exemplify the hybrid precoding by introducing a single user hybrid precoding structure of full connection in detail.

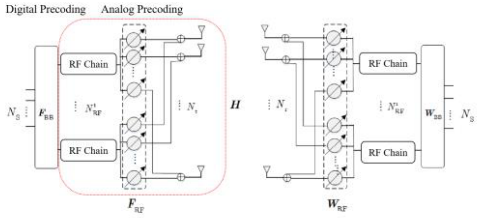

Figure 1. Hybrid Precoding System Model for Fully Connected Single User

As shown in Figure 1., we consider a fully connected single user hybrid precoding system model. The transmitter has N_t transmitting antennas and N_t^{RF} RF chains, and the receiver has N_r receiving antennas and the same N_t^{RF} RF chains as the transmitter.

The transmitter utilizes digital baseband precoder F_{BB} to process the received original data stream $\mathbf{s} \in \mathbb{C}^{N_s \times 1}$, where $E[\mathbf{s}\mathbf{s}^{\mathrm{H}}] = \mathbf{I}$. Then, the processed data stream is upconverted to the intermediate frequency using the RF link. Next, the intermediate

frequency data stream is processed by analog precoder $\mathbf{F_{RF}}$. Finally, the processed data stream is transmitted over channel $\mathbf{H} \in \mathbb{C}^{N_r \times N_t}$ via transmitting antennas.

After receiving the signal, the antenna at the receiving end first utilizes the analog precoder $\mathbf{W_{RF}}$ to process the received signal, and then downconverts the intermediate-frequency signal to baseband using the RF link. Next, the signal is further processed with the digital baseband precoder $\mathbf{W_{BB}}$. Finally, the received signal at the receiver is given by

$$\begin{aligned} \hat{\mathbf{s}} &= \mathbf{W}_{\mathbf{BB}}^{\mathrm{H}} \mathbf{W}_{\mathbf{RF}}^{\mathrm{H}} \mathbf{y} \\ &= \mathbf{W}_{\mathbf{BB}}^{\mathrm{H}} \mathbf{W}_{\mathbf{RF}}^{\mathrm{H}} \mathbf{H} \mathbf{F}_{\mathbf{RF}} \mathbf{F}_{\mathbf{BB}} \mathbf{s} + \mathbf{W}_{\mathbf{BB}}^{\mathrm{H}} \mathbf{W}_{\mathbf{RF}}^{\mathrm{H}} \mathbf{n} \end{aligned} . \tag{1}$$

Accordingly, the achievable rate of the hybrid precoding system can be expressed as

$$R = \log \det \left(\mathbf{I} + \frac{\mathbf{W}_{\mathbf{BB}}^{\mathrm{H}} \mathbf{W}_{\mathbf{RF}}^{\mathrm{H}} \mathbf{H} \mathbf{F}_{\mathbf{RF}} \mathbf{F}_{\mathbf{BB}} \mathbf{F}_{\mathbf{BB}}^{\mathrm{H}} \mathbf{F}_{\mathbf{RF}}^{\mathrm{H}} \mathbf{H}^{\mathrm{H}} \mathbf{W}_{\mathbf{RF}} \mathbf{W}_{\mathbf{BB}}}{\sigma^2 \mathbf{W}_{\mathbf{BB}}^{\mathrm{H}} \mathbf{W}_{\mathbf{RF}}^{\mathrm{H}} \mathbf{W}_{\mathbf{RF}} \mathbf{W}_{\mathbf{BB}}} \right). \tag{2}$$

2.2. Channel Model

We adopt extended Saleh Valenzuela (S-V) channel model [9,10] in this paper, where the signal transmitted from the base station will reach the user after a finite number of scatterings.

This model assumes that the number of scattering clusters is N_{cl} with each cluster containing N_{ray} transmission paths, and the inequality $N_{RF}^t \le N_{cl} N_{ray} \le \min(N_t, N_r)$ should be satisfied. Here, N_{RF}^t is the number of RF links at the transmitter, $\min(\bullet)$ is the obtained minimum, and N_t, N_r are the number of antennas at the transmitter and receiver, respectively. As a result, the narrowband discrete-time channel matrix [11] can be expressed as

$$\mathbf{H} = \sqrt{\frac{N_t N_r}{N_{cl} N_{ray}}} \sum_{i=1}^{N_{cl}} \sum_{l=1}^{N_{ray}} \alpha_{i,l} \mathbf{a_r}(\theta_{i,l}^r \varphi_{i,l}^r) \mathbf{a_t}(\theta_{i,l}^t \varphi_{i,l}^t)^{\mathrm{H}}, \tag{3}$$

where independent and identically distributed $\alpha_{i,l}$ is the gain coefficient of the l-th transmission path of the i-th cluster yielding zero mean and $\sigma_{\alpha,i}^2$ variance, where $\sigma_{\alpha,i}^2$ is the average power of the i-th cluster. $\mathbf{a_r}(\theta_{i,l}^r \varphi_{i,l}^r)$ and $\mathbf{a_t}(\theta_{i,l}^t \varphi_{i,l}^t)$ represent the response vector of antenna arrays at the receiver and transmitter, respectively. $(\bullet)^H$ denotes the conjugate transposition of a vector. $\theta_{i,l}^r \in [0, 2\pi)$ and $\theta_{i,l}^t \in [0, 2\pi)$ are the horizontal arrival angle and departure angle of the l-th transmission path of the i cluster, respectively. Similarly, $\varphi_{i,l}^r \in [0, 2\pi)$ and $\varphi_{i,l}^t \in [0, 2\pi)$ denote the vertical arrival angle and departure angle of the l-th transmission path of cluster i, respectively.

In this paper, the antenna arrays at the transceivers are considered to be uniform square planar array (USPA)[8]. For a typical uniform planar array with $\sqrt{N}$ horizontal elements and $\sqrt{N}$ vertical elements, $a(\varphi, \theta)$ satisfies the following conditions:

$$\mathbf{a}(\varphi,\theta)=\frac{1}{N}\left[1,...,e^{j2\pi\frac{d}{\lambda}(m\sin(\varphi)\sin(\theta)+n\cos(\theta))},...,e^{j2\pi\frac{d}{\lambda}((\sqrt{N}-1)\sin(\varphi)\sin(\theta)+(\sqrt{N}-1)\cos(\theta))}\right]^T, \quad (4)$$

where λ is the single wave wavelength. For a uniform planar array, d_1 and d_2 are the horizontal and vertical spacing of the antennas, respectively. We suppose that $d=d_1=d_2=\lambda/2$ is satisfied for the considered millimeter wave settings.

2.3. Optimization Problem

With reference to [12,13], the formulated problem can be expressed as

$$\begin{aligned}&\min_{\mathbf{F_{BB}},\mathbf{F_{RF}}}\left\|\mathbf{F_{opt}}-\mathbf{F_{RF}}\mathbf{F_{BB}}\right\|_F\\ &s.t.\quad \mathbf{F_{RF}}\in f_{RF}\\ &\qquad\left\|\mathbf{F_{RF}}\mathbf{F_{BB}}\right\|_F=N_s\end{aligned} \quad (5)$$

where f_{RF} is the set of all feasible simulated beam vectors.

3. Precoding Matrix Design

In a nutshell, the main task for designing a precoder is to solve a matrix factorization problem while satisfying specific constraints, as shown in equation (4).

In the hybrid precoding scheme, the columns in the digital precoding matrix are orthogonal with each other, which can be rewritten as

$$\mathbf{F}_{\mathbf{BB}}^{\mathrm{H}}\mathbf{F_{BB}}=\alpha\mathbf{I}_{\mathbf{N_s}}. \quad (6)$$

Then, it is plausible to fix the digital precoding matrix and then obtain the optimal solution of analog precoding according to the least square criterion. Based on the analysis, the problem can be described as

$$\arg_{\mathbf{F_{RF}}}\mathbf{F_{opt}}=\mathbf{F_{RF}}\mathbf{F_{BB}},\mathbf{F_{RF}}\in f_{RF}. \quad (7)$$

The matrix $\mathbf{F_{opt}}=\mathbf{F_{RF}}\mathbf{F_{BB}}$ in (7) can be transformed as

$$\mathbf{F_{opt}}\mathbf{I}_{\mathbf{N_s}}=\mathbf{F_{RF}}\mathbf{I}_{\mathbf{N_s}}\mathbf{F_{BB}}. \quad (8)$$

Right multiplying $\mathbf{F}_{\mathbf{BB}}^{\mathrm{H}}$ at the both sides of equation (8), equation (6) is rewritten as

$$\mathbf{F_{opt}}\mathbf{F}_{\mathbf{BB}}^{\mathrm{H}}=\alpha\mathbf{F_{RF}}\mathbf{I}_{\mathbf{N_s}}. \quad (9)$$

Based on equation (9), the analog precoding matrix can be obtained as

$$\mathbf{F_{RF}}=\frac{\mathbf{F_{opt}}\mathbf{F}_{\mathbf{BB}}^{\mathrm{H}}}{\alpha}. \quad (10)$$

Because of the modular constraint of $\mathbf{F_{RF}}$, the analog precoding matrix can be written as

$$\mathbf{F_{RF}}=\exp(i\bullet\arg\{\mathbf{F_{opt}}\mathbf{F}_{\mathbf{BB}}^{\mathrm{H}}\}). \quad (11)$$

Considering that the columns in the digital precoding are orthogonal to each other, we can finally find $\mathbf{F_{RF}}$ based on equation (11), as given by

$$\mathbf{F_{RF}}=\exp(i\bullet\arg\{\mathbf{F_{opt}}(\mathbf{F_{BB}})^{-1}\}). \quad (12)$$

Accordingly, the digital precoding matrix can be solved by the following least square method:

$$\mathbf{F}_{\mathbf{BB}} = (\mathbf{F}_{\mathbf{RF}}^{\mathrm{H}}\mathbf{F}_{\mathbf{RF}})^{-1}\mathbf{F}_{\mathbf{RF}}^{\mathrm{H}}\mathbf{F}_{\mathbf{opt}} . \tag{13}$$

Based the above analysis, the calculation formulas of digital precoding matrix and analog precoding matrix can be obtained, so the iterative solution can be obtained by alternating minimization method.

4. Algorithm Design

Firstly, the analog precoding matrix and the digital precoding matrix are obtained by preprocessing the orthogonal matching pursuit algorithm. Then, the analog precoding matrix is updated by the phase information extracted from the digital precoding matrix and the optimal digital precoding matrix. Finally, the local optimal solution is iteratively obtained under the least square criterion and modulus constraint.

The implementation process of AIPO algorithm is summarized in Algorithm 1.

Algorithm 1: Alternating Minimization of Inverse Matrix of Phase Extraction based on Orthogonal Matching Pursuit (AIPO) Hybrid Precoding Algorithm:

Require: $\mathbf{F}_{\mathbf{opt}}$, $\mathbf{A}_{\mathbf{t}}$, N_{RF}^{t}

Initialization: $\mathbf{F}_{\mathbf{RF}} = 0_{N_t \times N_{RF}^t}$, $\mathbf{F}_{\mathrm{BB}} = 0_{N_{RF}^t \times N_s}$, $k = 0$, $\mathbf{F}_{\mathbf{res}} = \mathbf{F}_{\mathbf{opt}}$;

1: **for** $i = 1 : N_{RF}^{t}$ **do**

2: Get analog precoding vector $\mathbf{F}_{\mathbf{RF}}^{i}$:count $\boldsymbol{\Psi} = \mathbf{A}_{\mathbf{t}}^{\mathrm{H}}\mathbf{F}_{\mathbf{res}} \rightarrow \mathbf{F}_{\mathbf{RF}}^{\mathrm{i}} = \mathbf{A}_{\mathbf{t}}^{(\arg \max_{l=1,2,\ldots,N_{cl}N_{ray}} \left(\boldsymbol{\Psi}\boldsymbol{\Psi}^{\mathrm{H}}\right)_{l,l})}$;

3: Update analog precoding matrix: $\mathbf{F}_{\mathbf{RF}} = \left[\mathbf{F}_{\mathbf{RF}} \mid \mathbf{F}_{\mathbf{RF}}^{\mathrm{i}}\right]$;

4: Update digital precoding matrix: $\mathbf{F}_{\mathbf{BB}} = \left(\mathbf{F}_{\mathbf{RF}}^{\mathrm{H}}\mathbf{F}_{\mathbf{RF}}\right)^{-1}\mathbf{F}_{\mathbf{RF}}^{\mathrm{H}}\mathbf{F}_{\mathbf{opt}}$;

5: Update residual matrix: $\mathbf{F}_{\mathbf{res}} = \dfrac{\mathbf{F}_{\mathbf{opt}} - \mathbf{F}_{\mathbf{RF}}\mathbf{F}_{\mathbf{BB}}}{\left\|\mathbf{F}_{\mathbf{opt}} - \mathbf{F}_{\mathbf{RF}}\mathbf{F}_{\mathbf{BB}}\right\|_F}$;

6: **end for**

7: Normalized digital precoding matrix: $\mathbf{F}_{\mathbf{BB}} = \sqrt{N_s}\dfrac{\mathbf{F}_{\mathbf{BB}}}{\left\|\mathbf{F}_{\mathbf{RF}}\mathbf{F}_{\mathbf{BB}}\right\|_F}$;

8: **while** the iteration condition is satisfied **do**

9: Update the analog precoding matrix: $\arg\{\mathbf{F}_{\mathbf{RF}}^{(k+1)}\} = \arg\{\mathbf{F}_{\mathbf{opt}}(\mathbf{F}_{\mathbf{BB}})^{-1}\}$, where $\arg\{\bullet\}$ is the phase information of the matrix.

10: Update digital precoding matrix: $\mathbf{F}_{\mathbf{BB}} = \left(\mathbf{F}_{\mathbf{RF}}^{\mathrm{H}}\mathbf{F}_{\mathbf{RF}}\right)^{-1}\mathbf{F}_{\mathbf{RF}}^{\mathrm{H}}\mathbf{F}_{\mathbf{opt}}$;

11: $k = k + 1$;

12: **end while**

13: Normalized digital precoding matrix: $\mathbf{F}_{\mathbf{BB}} = \sqrt{N_s}\dfrac{\mathbf{F}_{\mathbf{BB}}}{\left\|\mathbf{F}_{\mathbf{RF}}\mathbf{F}_{\mathbf{BB}}\right\|_F}$.

14: **Return**: $\mathbf{F}_{\mathbf{RF}}$, $\mathbf{F}_{\mathbf{BB}}$

5. Simulation Result and Algorithm Complexity Analysis

5.1. Simulation Setup

The simulation parameters are listed in Table 1.

Table 1. Simulation Parameters

Parameter name	Parameter value
Number of transmitting antennas N_t	256
Number of receiving antennas N_r	36
Antenna spacing d	λ/2
Number of clusters N_{cl}	5
Number of scatterers N_{ray}	10
Average power of clusters	1
Average power of transmitter P_{common}	10W
RF link power P_{RF}	100mW
Phasor power P_{PS}	10mW
Power amplifier power P_{PA}	100mW

5.2. Simulation Performance Analysis

For comparison, we consider the PE-AltMin algorithm proposed in reference [14] and OMP-PE-AltMin algorithm initialized by OMP as benchmarks.

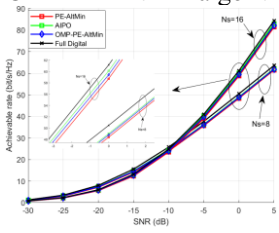

Figure 2. Spectrum Efficiency Curves with the Change of SNR.

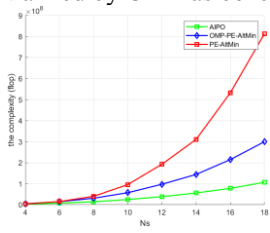

Figure 3. Algorithm Complexity Curves under Different Data Stream Numbers.

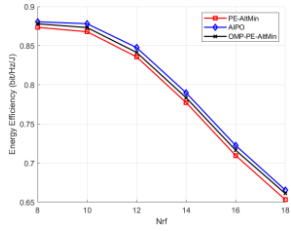

Figure 4. Energy Efficiency Curves under Different Data Stream Numbers.

In Figure 2, we show the spectrum efficiency versus SNR values of AIPO, PE-AltMin, optimal pure digital precoding, and OMP-PE-AltMin. The number of RF links at the base station and the receiving end equal to the number of data streams, i.e., $N_s = N_{RF}^t = N_{RF}^r = \{ 8, 16 \}$ .It can be seen that the AIPO algorithm proposed in this paper achieves comparable achievable rate to the optimal pure digital precoding. Moreover, AIPO outperforms both PE-AltMin and OMP-PE-AltMin.

In Figure 3, we show the algorithm complexity of AIPO and the benchmarks under different data stream numbers, i.e. $N_s = N_{RF}^t = N_{RF}^r = \{ 4, 6, 8, 10, 12, 14, 16, 18 \}$ .It is obtained that the algorithm complexity of the proposed AIPO is much lower than that of the benchmarks. This effectively validates the viability of AIPO.

In Figure 4, we plot the energy efficiency of AIPO and the benchmarks under different data stream numbers, i.e., $N_s = N_{RF}^t = N_{RF}^r = \{ 8, 10, 12, 14, 16, 18 \}$. It is

obtained that the energy efficiency of AIPO is significantly higher than PE-AltMin and OMP-PE-AltMin. Therefore, the proposed AIPO is capable of preserving more energy.

5.3. Complexity Analysis

In this paper, the AIPO algorithm is initialized by OMP, and then the analog precoding matrix is obtained by updating the phase information of the digital precoding matrix and the optimal precoding matrix. Based on the obtained analog precoding matrix, the digital precoding matrix is updated according to the least square criterion. The digital precoding matrix and the analog precoding matrix will be iteratively updated until the predefined convergence conditions are satisfied.

The complexity of OMP initialization algorithm is summarized in Table 2. The complexity of AIPO iterative algorithm is concluded in Table 3. The complexity of PE-Altmin iterative algorithm is shown in Table 4.

Table 2. The Complexity of OMP [1] Initialization Algorithm, where $L = N_{cl} \times N_{ray}$

Step	Operation	Complexity
1	$\mathbf{\Psi} = \mathbf{A}_t^{\mathrm{H}} \mathbf{F}_{\mathrm{res}}$	$8LN_tN_s$
2	$k = \arg \max_{l=1,2,\ldots,N_{cl}N_{ray}} \left(\mathbf{\Psi}\mathbf{\Psi}^{\mathrm{H}}\right)_{l,l}$	$8L^2N_s$
3	$\mathbf{F}_{\mathbf{BB}} = \left(\mathbf{F}_{\mathbf{RF}}^{\mathrm{H}}\mathbf{F}_{\mathbf{RF}}\right)^{-1}\mathbf{F}_{\mathbf{RF}}^{\mathrm{H}}\mathbf{F}_{\mathbf{opt}}$	$2N_{RF}^{t\,3} - 2N_{RF}^{t\,2} + N_{RF}^t + 8N_{RF}^{t\,2}N_t + 8N_tN_{RF}^tN_s$
4	$\mathbf{F}_{\mathbf{res}} = \dfrac{\mathbf{F}_{\mathbf{opt}} - \mathbf{F}_{\mathbf{RF}}\mathbf{F}_{\mathbf{BB}}}{\left\|\mathbf{F}_{\mathbf{opt}} - \mathbf{F}_{\mathbf{RF}}\mathbf{F}_{\mathbf{BB}}\right\|_F}$	$8N_tN_{RF}^tN_s + 2N_tN_s$

Table 3. The Complexity of AIPO Iterative Algorithm

Step	Operation	Complexity
1	$\arg\{\mathbf{F}_{\mathbf{RF}}^{(k+1)}\} = \arg\{\mathbf{F}_{\mathbf{opt}}(\mathbf{F}_{\mathbf{BB}})^{-1}\}$	$N_tN_{RF}^t + 8N_tN_{RF}^tN_s$
2	$\mathbf{F}_{\mathbf{BB}} = \left(\mathbf{F}_{\mathbf{RF}}^{\mathrm{H}}\mathbf{F}_{\mathbf{RF}}\right)^{-1}\mathbf{F}_{\mathbf{RF}}^{\mathrm{H}}\mathbf{F}_{\mathbf{opt}}$	$2N_{RF}^{t\,3} - 2N_{RF}^{t\,2} + N_{RF}^t + 8N_{RF}^{t\,2}N_t + 8N_tN_{RF}^tN_s$

Table 4. The Complexity of PE-Altmin [8] Iterative Algorithm

Step	Operation	Complexity
1	$\mathbf{\Psi} = \left(\mathbf{F}_{\mathbf{opt}}\right)^{\mathrm{H}}\mathbf{F}_{\mathbf{RF}}^{(k)}$	$8N_tN_{RF}^tN_s$
2	$\mathbf{\Psi} = \mathbf{U}^{(k)}\mathbf{\Sigma}^{(k)}\left(\mathbf{V}^{(k)}\right)^{\mathrm{H}}$	$72N_s^3 + 64N_{RF}^tN_s^2 + 32N_{RF}^{t\,2}N_s$
3	$\mathbf{F}_{\mathbf{BB}}^{(k)} = \mathbf{V}^{(k)}(,1:N_s)\left(\mathbf{U}^{(k)}\right)^{\mathrm{H}}$	$8N_{RF}^tN_s^2$
4	$\arg\{\mathbf{F}_{\mathbf{RF}}^{(k+1)}\} = \arg\{\mathbf{F}_{\mathbf{opt}}\left(\mathbf{F}_{\mathbf{BB}}^{(k)}\right)^{\mathrm{H}}\}$	$N_tN_{RF}^t + 8N_tN_{RF}^tN_s$

In Table 5, it is seen that AIPO not only achieves better performance than PE-AltMin and OMP-PE-AltMin, but requires much fewer iterations than the benchmarks to reach convergence. Quantitatively speaking, the proposed AIPO complexity is reduced by 66.90% regarding PE-AltMin and 86.32% regarding OMP-PE-AltMin.

Table 5. Comparison of required iterations, where $N_s = N_{RF}^t = N_{RF}^r = 18$

Algorithm	Initialization complexity	Single iteration complexity	Average number of iterations	Total complexity
AIPO	75853908	2006298	14.79	1.0553×10^8
OMP-PE-AltMin	75853908	2358144	103.0506	3.1886×10^8
PE-AltMin	4608	2358144	327.2079	7.71118×10^8

6. Conclusion

This paper investigated the problem of hybrid precoding for single user millimeter wave MIMO systems. We proposed AIPO hybrid precoding algorithm to solve the formulated problem. The proposed AIPO enjoyed significant improvement in both spectrum and energy efficiency, which achieved performance close to pure digital precoding algorithm. Besides, the complexity of the algorithm was far less than state-of-the-art benchmarks. Simulation results validated that AIPO can be effectively utilized as a hybrid precoding solution with relatively low complexity and satisfactory performance.

The algorithm proposed in this paper is not significant for the improvement of algorithm complexity when the system performance requirement is not high. In the future, we will focus on the computational complexity optimization for the case of relaxed iteration requirements.

Acknowledgements

This work was supported by the National Natural Science Foundation of China (NSFC,No.61531007)

References

[1] Ayach O E, Rajagopal S, Abu-Surra S, et al. Spatially sparse precoding in millimeter wave MIMO systems. IEEE Transactions on Wireless Communications, 2014, 13(3):1499-1513.

[2] M. A. Azam, A. K. Dutta and A. Mukherjee. Downlink Precoding for Hybrid Fully Connected Linear Subarrays in mmWave With Rainfall Scattering and Hardware Impairments. IEEE Transactions on Vehicular Technology, 2022, 71(5):5143-5155.

[3] X. Qiao, Y. Zhang, H. Cao, Z. Xu and L. Yang. Hybrid Precoders and Combiners for Sub- Connected and Fully Connected Structures. IEEE International Conference on Consumer Electronics - Taiwan (ICCE-TW), 2019:1-2.

[4] X. Liu, W. Chen and J. Chu. Behavioral Modeling and Digital Predistortion for Fully-Connected Hybrid Beamforming Massive MIMO Transmitters. 2020 IEEE Asia-Pacific Microwave Conference (APMC), 2020:463-465.

[5] Sohrabi Foad, Yu Wei. Hybrid digital and analog beamforming design for Large-scale antenna arrays. IEEE Journal of Selected Topics in Signal Processing, 2016, 10(3):501-513.

[6] A. Osama, M. Elsaadany, S. I. Shams, A. M. A. Omar, U. S. Mohammed and G. Gagnon. Hybrid Precoder Design for mmWave Massive MIMO Systems with Partially Connected Architecture. International Symposium on Networks, Computers and Communications (ISNCC), 2021:1-6.

[7] L. Pang et al. Iterative Hybrid Precoding and Combining for Partially-Connected Massive MIMO mmWave Systems. IEEE 92nd Vehicular Technology Conference (VTC2020-Fall), 2020:1-5.

[8] X. Yu, J. Shen, J. Zhang and K. B. Letaief. Alternating Minimization Algorithms for Hybrid Precoding in Millimeter Wave MIMO Systems," in IEEE Journal of Selected Topics in Signal Processing, vol. 10, no. 3, pp. 485-500, April 2016.

[9] Alkhateeb A, Ayach O E, Leus G, et al. Channel estimation and hybrid precoding for millimeter wave cellular systems. IEEE Journal of Selected Topics in Signal Processing, 2014, 8(5):831-846.

[10] Bai T, Alkhateeb A, Heath R W. Coverage and capacity of millimeter-wave cellular networks. IEEE Communications Magazine, 2014, 52(9):70-77.

[11] Samimi M K, Rappaport T S. 3-D statistical channel model for millimeter-wave outdoor mobile broadband communications. IEEE International Conference on Communications. London, UK: IEEE Press, 2015:2430-2436.

[12] O. El Ayach, S. Rajagopal, S. Abu-Surra, Z. Pi, and R. W. Heath. Spatially sparse precoding in millimeter wave MIMO systems. IEEE Trans. Wireless Commun., 2014, 13(3):1499–1513.

[13] Y. Lee, C. Wang, and Y. Huang. A hybrid RF/baseband precoding processor based on parallel-index-selection matrix-inversion-bypass simultaneous orthogonal matching pursuit for millimeter wave MIMO systems. IEEE Trans. Signal Process., 2015, 63(2):305–317.